



Geochemistry Signature and K-Ar Age of the I-type Granite at East Coast of Bangka Island

RONALDO IRZON¹, MUHAMMAD ZULFIKAR², UDAYA KAMILUDIN², NOOR CAHYO DWI ARYANTO³,
DENY SETIADI², YOGI NOVIADI³, and UNDANG HERNAWAN⁴

¹Center for Geological Survey Indonesia, Jln. Diponegoro 57 Bandung, West Java

²Marine Geological Institute Indonesia, Jln. Dr. Djunjunan 236 Bandung, West Java

³Research Center for Geological Resources, Cisitua-Sangkuriang, Bandung, West Java

⁴Research Center for Oceanography, Jln Pasir Putih Raya No. 1, Pademangan, Jakarta

Corresponding author: ronaldoirzon18@gmail.com

Manuscript received: May, 13, 2022; revised: April, 5, 2023;

approved: July, 3, 2023; available online: September, 25, 2023

Abstract - This work presents microscopic-, whole-rock geochemical-, and K-Ar age data for Tanjung Berikat Granitoid at the easternmost part of Bangka Island. Some selected samples are in the range of monzogranite and granodiorite based on microscopic analysis. The rocks are characterized by a wide range in SiO₂ (62.75 - 70.17 wt %), high-K calc-alkaline to shoshonitic affinity, and ferroan signature. Very good correlation values of bivariate SiO₂ plotted against other major oxides, similar spider diagrams normalized to the composition of the N-MORB and chondrite-normalized REE diagrams demonstrate the same origin and crystallization mechanism of the granitoid. The I-type nature of the studied granite is based on the hornblende existence, metaluminous character, negative SiO₂ to P₂O₅ correlation, and volcanic arc characteristics of the rock. Tanjung Berikat Granitoid was crystallized in the mid-late Early Cretaceous at 125.5 ± 2.8 Ma and 109.4 ± 2.5 Ma based on the K-Ar dating method.

Keywords: granitoid, geochemistry, I-type, Bangka Island

© IJOG - 2023

How to cite this article:

Irzon, R., Zulfiakar, M., Kamiludin, U., Aryanto, N.C.D., Setiadi, D., Noviadi, Y., and Hernawan, U., 2023. Geochemistry Signature and K-Ar Age of the I-type Granite at East Coast of Bangka Island. *Indonesian Journal on Geoscience*, 10 (3), p.309-322. DOI: [10.17014/ijog.10.3.309-322](https://doi.org/10.17014/ijog.10.3.309-322)

INTRODUCTION

Background

Tectonic history of the Southeast Asia region which is composed of continental blocks, namely Sibumasu, Indochina, East Malaya, West Sumatra, West Burma, Simao, and Southwest Borneo is enigmatic (*i.e.* Barber and Crow, 2009; Metcalfe 2011, 2013; Hall and Sevastjanova, 2012; Cottam *et al.*, 2013; Breitfeld *et al.*, 2017; Ng *et al.*, 2017; Hazad *et al.*, 2019; Irzon *et al.*, 2021). Classification of granitic rocks of Southeast Asia into Eastern, Main Range, and Western Provinces is based on continental

blocks convergences with several ancient oceans called Palaeo-Tethys, Meso-Tethys, and Cenozoic Tethys (Barber, 2000; Barber and Crow, 2003; Metcalfe, 2011, 2013; Jiang *et al.*, 2017; Irzon *et al.*, 2022). The detachment of North China, South China, Indochina, and East Malaya Blocks from the mainland Gondwana through Early Devonian opened the Palaeo-Tethys (Metcalfe, 2011). Cimmerian continent, including Bashoan, Tengchong, and Sibumasu, then moved away from Gondwana in Early Permian to open the Meso-Tethys. Eastern Granite Province was initiated by the subduction of Palaeo-Tethys below Indochina (including East Malaya) since

Permian (Searle *et al.*, 2012; Metcalfe, 2013). After the closing of Paleo-Tethys, the Main Range Province magmatism was initiated because of the Sibumasu and Indochina collision (Metcalfe, 2011; Metcalfe, 2013). Previous studies indicated that the heat for Western Granite Province magmatism should have come from the Ceno-Tethys subduction beneath West Phuket and Mogok Belts in Burma (Searle *et al.*, 2012; Setiawan *et al.*, 2017). Granitoid provinces in Southeast Asia region are given in Figure 1.

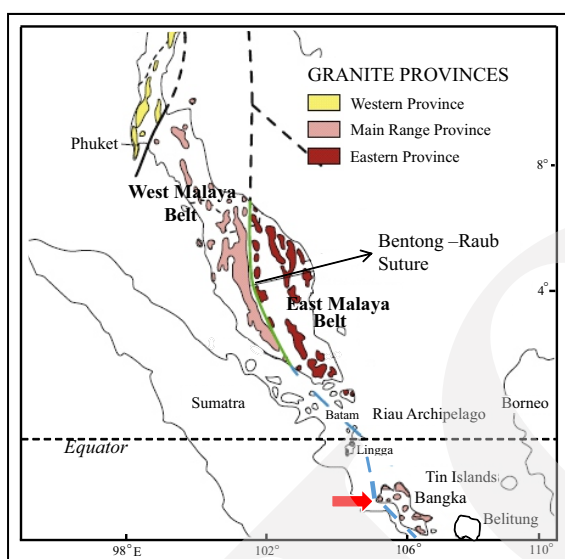


Figure 1. Eastern, Main Range, and Western Granite Provinces of Southeast Asia (modified after Cobbing (2005) and Metcalfe (2011)).

Most granitoid intrusions of the Eastern Province located in Thailand, eastern region of Malaysia, at several islands in the east of Sumatra, and in East Kalimantan are I-type, volcanic-arc correlated, and hornblende-bearing rocks (Ghani, 2000; Ghani *et al.*, 2013; Irzon, 2017; Kazemi *et al.*, 2019; Hazad *et al.*, 2019; Irzon *et al.*, 2020). The Main Range Province is coherent with the Western Granite Belt of Malay Peninsula. Giant tin deposits in Bangka, Belitung, and Kinta Valley occur along with the majority of S-type granites in the Main Range Province (Cobbing, 2005; Jamil *et al.*, 2016; Ng *et al.*, 2017). Both I- and S-type granites are identified in the Western Province of Burma and western Thailand. However, Clarke and Beddoe-Stephens (1987)

argued that Hatapang Granite in North Sumatra should also belong to the youngest province according to similar microscopic and geochemistry characteristics.

As discussed above, Bangka Island belongs to the tin islands along with Bintan, Singkep, and Kundur (Ko, 1986; Ng *et al.*, 2017; Irzon *et al.*, 2022). A previous study illustrated that the stanniferous S-type granites in Bangka intruded during Triassic, are characterized by south-westward younging which might be the result of subduction roll-back (Ng *et al.*, 2017). However, the occurrence of several I-type intrusions on the island is puzzling and needs to be explained. This study aims to describe I-type granite in Tanjung Berikat, at the easternmost of Bangka considering its microscopic and geochemical characteristics. A total of seven granite samples were collected and analyzed. Three samples were analyzed for major, trace, and REE, while two of the samples were dated using the K-Ar method for the rock formation mechanism. However, the K-Ar age of magmatic rocks is not the same as the age of magma emplacement mechanism of the previous studies (*i.e.* Ng *et al.*, 2017; Siregar *et al.*, 2022).

Geological and Stratigraphical Settings

The geology of Bangka Island is published into two maps, namely the North Bangka Quadrangle (Mangga and Djamal, 1994) and the South Bangka Quadrangle (Margono *et al.*, 1995). Tanjung Berikat is situated on the west coast of the South Bangka Quadrangle. Pemali Metamorphic Complex which is composed of phyllite, schist, and quartzite was formed in the latest Carboniferous to Permian age (Margono *et al.*, 1995). Tanjung Genting Formation formed in Triassic consists of alternating sandstone and claystone. Both of the sedimentary rocks are fine- to medium-grained and well-sorted, with local lenses of limestone.

Different granitoid rocks in Bangka intruding the Tanjung Genting Formation were classified into biotite granite, granodiorite, and gneissic granite (Margono *et al.*, 1995). A study discussing granitic rocks in Bangka explained that the rocks

were crystallized during Late Triassic (229.9 - 204.4 Ma) using U-Pb dating (Ng *et al.*, 2017). The plutonic rocks are trending E–W, elongated in shape, and can be discriminated into biotite granites and hornblende-biotite granodiorites (Ko, 1986). The first type is coherent with S-type granites, while the second one is with I-type. Tin mineralization in Bangka is linked to peraluminous tin-bearing S-type granites which typically spread in the main granite province of Southeast Asia (Cobbing 2005; Irzon *et al.*, 2018). Based on its geochemical composition, a previous study predicted that titanite and malayaite present together in the tin-bearing granites of Nudur at southern Bangka (Irzon *et al.*, 2020). A total of ten samples were collected in the frame of the fieldwork in Tanjung Berikat, at Bangka Island (Figure 2).

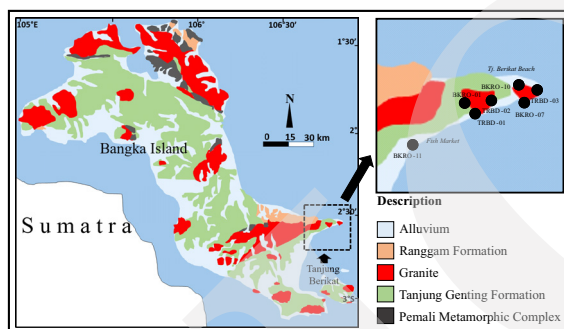


Figure 2. Geological map of Bangka and sample locations, modified from Mangga and Djamal (1994) and Margono *et al.* (1995). Tanjung Berikat is located at the eastmost of the tin island.

TRBD-03, BKRO-07, and BKRO-10 are three granitic rocks that outcrop nearby Tanjung Berikat Beach (Figure 2). The samples are light grey, holocrystalline, phaneritic granitoid, and very coarse-grained rocks. Xenoliths of mafic volcanic rock with a diameter of 5 - 20 cm are common in all studied outcrops. The other four intrusive rocks TRBD-01, TRBD-02, BKRO-01, and BKRO-11 were taken not more than 300 m from the east of a fish market. These granite outcrops are relatively almost alike to the ones from Tanjung Berikat, but they show a more reddish colour.

Under the microscope, three of the selected igneous rocks are classified as granodiorite (BKRO-

01, BKRO-07, and BKRO-10), while another one is monzogranite (BKRO-11). Both groups are holocrystalline and equigranular (Figures 3a-d). The granodiorite is characterized by perthite texture, whilst monzogranite shows a graphic one. They predominantly comprise plagioclase (22.8 - 50%), quartz (25.2 - 32.8%), orthoclase (8.3 - 20%), biotite (4.7 - 18%), hornblende (up to 7.6%), and epidote (0.4 - 4.8%). Accessory minerals include subordinate apatite and zircon. Biotite is partly altered to chlorite (2 - 4.4%). A small number of secondary quartz was detected in BKRO-07 and BKRO-10.

ANALYTICAL METHOD

Geochemical and microscopic analyses were done in the laboratory of Centre for Geological Survey Indonesia in November 2017. The major oxide content of the samples was measured using Advant-X-Ray Fluorescent (XRF), while trace and rare earth elements were determined by Thermo X-Series Inductively Coupled Plasma – Mass Spectrometry (ICP-MS). Before chemical preparation, the samples were crushed and milled to attain the grain size of -200 mesh using a jaw crusher and ball mill. Pressed pellet method and acid destruction process were applied in XRF and ICP-MS analysis, respectively. The total volatiles in the samples pronounced on Lost of Ignition (LOI) was determined by weighing the dry sample and crucible, placing the sample in the crucible, heating in a furnace at 1,000°C, cooling in a desiccator, and re-weighing the residue in the crucible. Details for XRF and ICP-MS analytical procedures followed the previous works from Irzon and Abdullah (2016; 2018). Certified reference materials were also prepared and analyzed using the same process together with the samples for accuracy confirmation. All of the samples were analyzed using XRF. The data in this study is part of major geochemistry coastal mapping in Bangka, so only three representative samples were measured by ICP-MS. XRF and ICP-MS measurement results are shown in Table 1.

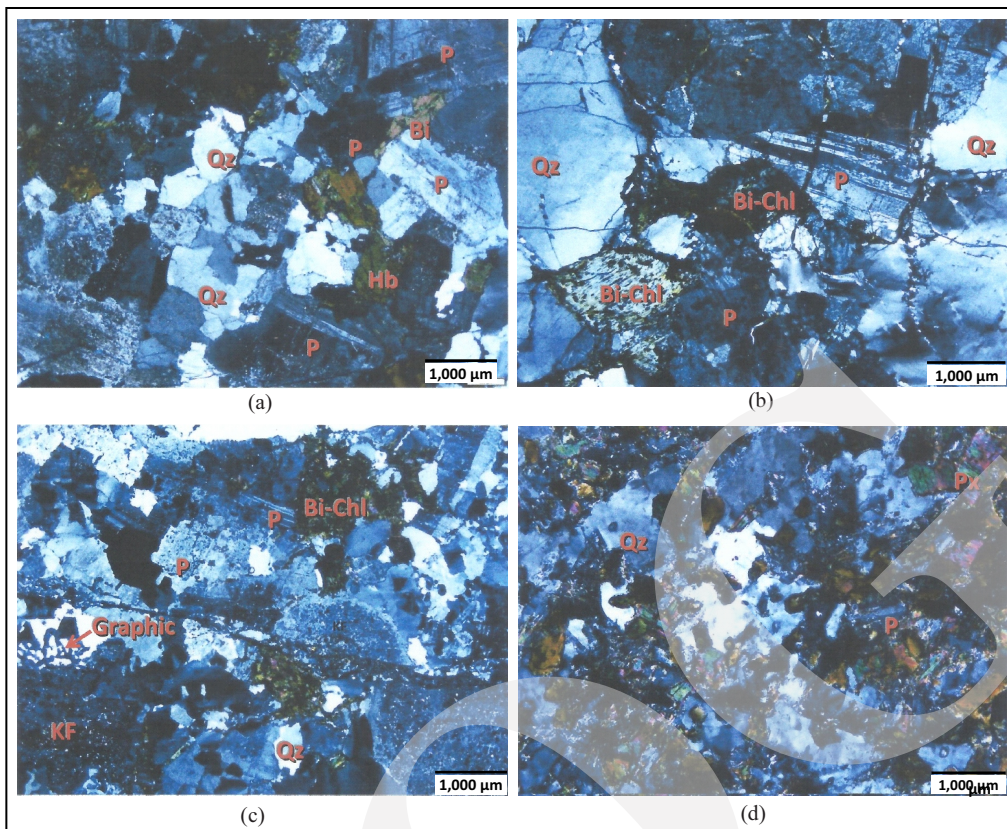


Figure 3. Photomicrographs of selected samples which majorly composed of quartz, plagioclase, K-feldspar, and hornblende. a) BKRO-01; b) BKRO-07; c) BKRO-10; and d) BKRO-11. Qz = quartz, Pl = plagioclase, KF = K-feldspar, Hb = hornblende, Px = pyroxene, Bi-Chl = biotite that have been replaced by chlorite, Sec Qz = secondary quartz.

Two of the selected samples (TRBD-01 and TRBD-03) were sent to Actlabs in Canada for K-Ar dating in January 2018. Splits of feldspar concentrate from the two samples were weighted into Al container, loaded into the sample system of extraction unit, and degassed at 100°C for two days to remove the surface gases. Argon was extracted in a double vacuum furnace at 1,700°C after the ^{38}Ar as the spike was introduced to the sample. Two-step purification schemes were adapted to clean up the extracted gases. Then pure Ar were introduced into a custom-built magnetic sector mass spectrometer. For all measurements in this study, 2σ defines the analytical error. Recommended decay constants of the previous study (Steiger and Jäger, 1977) with $\lambda_K = 0.581 \times 10^{-10} \text{y}^{-1}$, $\lambda_{\beta} = 4.962 \times 10^{-10} \text{y}^{-1}$, and $^{40}\text{K}/\text{K} = 0.01167$ (%) were applied for K-Ar age calculation. The K-Ar dating results are summarized in Table 2.

The discrimination between I-type and S-type granites was introduced based on an investiga-

tion of granites and related volcanic rocks in the Lachlan Fold Belt, eastern Australia. I-type granite is arc-related as the result of meta-igneous differentiation while S-type is collision-related and apparently of a metasedimentary source. The anorogenic A-type (Loiselle and Wones, 1979) and mantle-origin M-type (White, 1979; Pitcher, 1983) were proposed later. S-type granite is also called two-mica granite as it usually contains both biotite and muscovite (Ghani, 2000; Ghani *et al.*, 2013; Wang and Shu, 2012; Jamil *et al.*, 2016; Liu *et al.*, 2020). I-type intrusion is under-saturated in Al and particularly contains hornblende which is detected in the samples (Hazad *et al.*, 2019; Irzon *et al.*, 2020). SiO_2 to P_2O_5 correlation is useful for distinguishing I-type from S-type granites (Yanbo and Jingwen, 2010; Ghani *et al.*, 2013; Sarjoughian and Kananian, 2017; Irzon *et al.*, 2020). S-type intrusion depicts a positive SiO_2 to P_2O_5 correlation, whilst I-type with a negative one.

Table 1. Geochemistry Composition of the Studied Rocks. All samples are I-type granitoids

| Sample ID | Granitoid | | | | | | |
|-------------------------------------|---------------|---------------|------------------|---------|---------|---------|---------------|
| | TRBD-01 | TRBD-02 | TRBD-03 | BKRO-01 | BKRO-07 | BKRO-10 | BKRO-11 |
| Rock Name (after Middlemost, 1994) | Grano-diorite | Grano-diorite | Quartz-monzonite | Granite | Granite | Granite | Grano-diorite |
| Major oxides (%) | | | | | | | |
| SiO ₂ | 67.52 | 66.82 | 68.57 | 70.17 | 70.14 | 74.43 | 62.75 |
| TiO ₂ | 0.49 | 0.54 | 0.36 | 0.44 | 0.33 | 0.15 | 1.12 |
| Al ₂ O ₃ | 14.03 | 14.19 | 14.02 | 14.14 | 15.00 | 13.07 | 15.54 |
| Fe ₂ O _{3T} | 5.83 | 6.30 | 4.54 | 4.21 | 2.61 | 2.58 | 8.60 |
| MnO | 0.08 | 0.08 | 0.06 | 0.07 | 0.03 | 0.05 | 0.10 |
| CaO | 2.70 | 2.77 | 2.13 | 2.76 | 1.33 | 1.26 | 0.90 |
| MgO | 0.74 | 0.80 | 0.56 | 0.70 | 0.50 | 0.25 | 1.59 |
| Na ₂ O | 2.43 | 2.31 | 2.67 | 2.83 | 2.71 | 2.91 | 2.50 |
| K ₂ O | 4.71 | 4.71 | 6.05 | 4.17 | 5.80 | 5.16 | 2.56 |
| P ₂ O ₅ | 0.27 | 0.23 | 0.18 | 0.11 | 0.07 | 0.04 | 0.29 |
| LOI | 0.79 | 1.28 | 0.68 | 0.60 | 1.30 | 0.20 | 1.00 |
| Trace and rare earth elements (ppm) | | | | | | | |
| V | 216 | 227.2 | 257 | | | | |
| Ga | 3.96 | 10.36 | 4.62 | | | | |
| Rb | 18.72 | 23.01 | 9.95 | | | | |
| Sr | 1425 | 1099 | 1203 | | | | |
| Y | 20.54 | 18.53 | 24.88 | | | | |
| Nb | 20.46 | 25.95 | 25.24 | | | | |
| Ce | 96.31 | 106.6 | 99.84 | | | | |
| La | 39.89 | 47.91 | 45.36 | | | | |
| Pr | 11.84 | 12.29 | 11.49 | | | | |
| Nd | 37.36 | 36.65 | 34.83 | | | | |
| Sm | 5.2 | 4.83 | 4.33 | | | | |
| Eu | 1.98 | 1.89 | 1.81 | | | | |
| Gd | 6.08 | 5.62 | 5.43 | | | | |
| Tb | 1.14 | 0.96 | 0.91 | | | | |
| Dy | 4.58 | 4.12 | 4.07 | | | | |
| Ho | 1.18 | 0.99 | 1.02 | | | | |
| Er | 2.07 | 1.96 | 2 | | | | |
| Tm | 0.31 | 0.29 | 0.3 | | | | |
| Yb | 1.8 | 1.71 | 1.76 | | | | |
| Lu | 0.21 | 0.24 | 0.25 | | | | |
| Ta | 1.72 | 2.42 | 1.81 | | | | |
| Ti | 1.62 | 2.05 | 2.33 | | | | |
| Th | 27.2 | 33.78 | 38.25 | | | | |

Table 2. K-Ar Ages of Selected Samples from Tanjung Berikat Granitoid

| Sample ID | Separated Mineral | K±σ (%) | Rad. ⁴⁰ Ar (ng/g) | Rad. ⁴⁰ Ar Air (%) | Age (Ma) | Error (Ma) |
|-----------|-------------------|-----------|------------------------------|-------------------------------|----------|------------|
| TRBD-01 | feldspar | 4.58±0.05 | 41.27±0.13 | 6.1 | 125.5 | 2.8 |
| TRBD-03 | feldspar | 4.52±0.06 | 35.36±0.11 | 6.4 | 109.4 | 2.5 |

RESULTS

Major Oxides

As discussed above, four samples are confirmed as granitoid under the microscope analysis. On the QAP discrimination, the granitoid samples fall within monzogranite and granodiorite fields (Figure 4a). The studied igneous rocks are clearly

felsic with SiO₂ ranging from 62.75 to 74.43 wt. %. Al₂O₃ and Fe₂O_{3T} are the next abundant major oxides with the average compositions of 14.01 wt. % and 4.95 wt. %, respectively. The total alkali content varies from 5.57 to 8.72 wt. %. Data from previous studies in Bangka (Ng *et al.*, 2017, Schwartz *et al.*, 1995) were also used in this investigation for comparison. On the Total Alkali

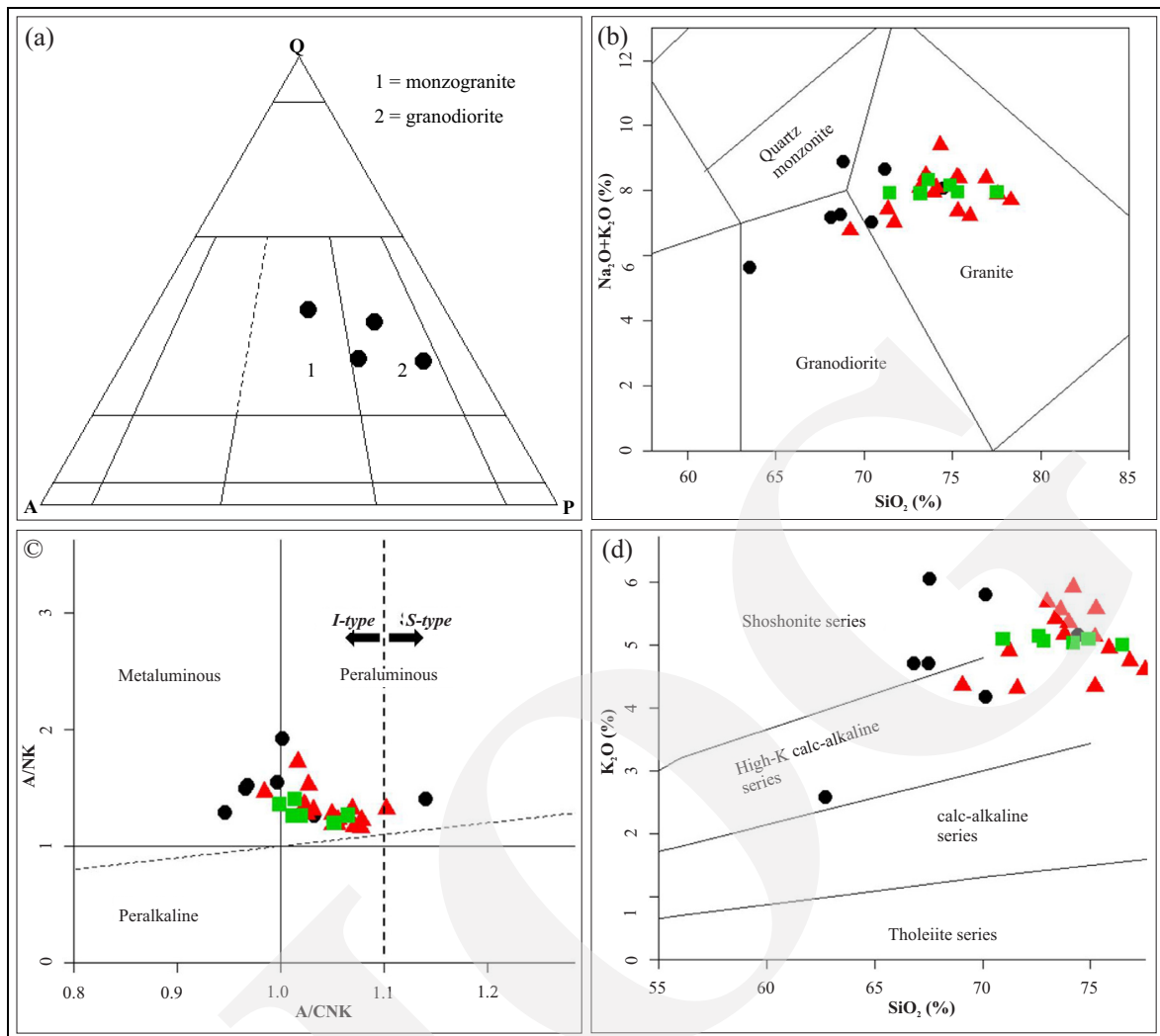


Figure 4. Plots of granitoids studied: a) QAP diagram (after Streckisen, 1976) explains that the samples are classified as granodiorite and monzogranite; b) Rocks fall within granodiorite, quartz-monzonite, and granite fields of TAS discrimination (after Middlemost, 1994); c) Plots of A/CNK vs. A/NK showing metaluminous to weakly peraluminous character of the granitoids; d) High potassium content of Tanjung Berikat Granitoid samples that fall in High-K calc-alkaline and shoshonite series on SiO_2 versus K_2O discrimination (after Peccerillo and Taylor, 1976). ● = Tanjung Berikat Granitoid, ■ = data from Schwartz *et al.* (1995), ▲ = data from Ng *et al.* (2017).

versus Silica (TAS) diagram, the samples are classified as granodiorite (three samples), quartz monzonite (one sample), and granite (three samples) as shown in Figure 4b. Most of the studied rocks show metaluminous to weakly peraluminous character in the A/CNK-A/NK binary plot (Figure 4c), implying molar alumina deficiency relative to total alkali and calcium. A high A/CNK value of one sample should correspond to a fractionated rock as discussed in previous works (*i.e.* Liu *et al.*, 2014; Choudhury and Hussain, 2021). The samples are highly potassic and correspond

to high-K calc-alkaline and shoshonite series in SiO_2 versus K_2O diagram as shown in Figure 4d. Based on their low LOI content (0.20 to 1.30 %), these rocks are fresh.

All seven studied granitoids are ferroan as shown in $\text{Fe}_2\text{O}_3/(\text{Fe}_2\text{O}_3+\text{MgO})$ versus SiO_2 wt. % diagram (Figure 5a). These samples are predominantly calc-alkalic to alkali-calcic on SiO_2 versus $\text{Na}_2\text{O}+\text{K}_2\text{O}-\text{CaO}$ diagram (Figure 5b). Pearce *et al.* (1984) proposed several diagrams associated with the granitoid tectonic environment based on several trace elements, where the stability field of

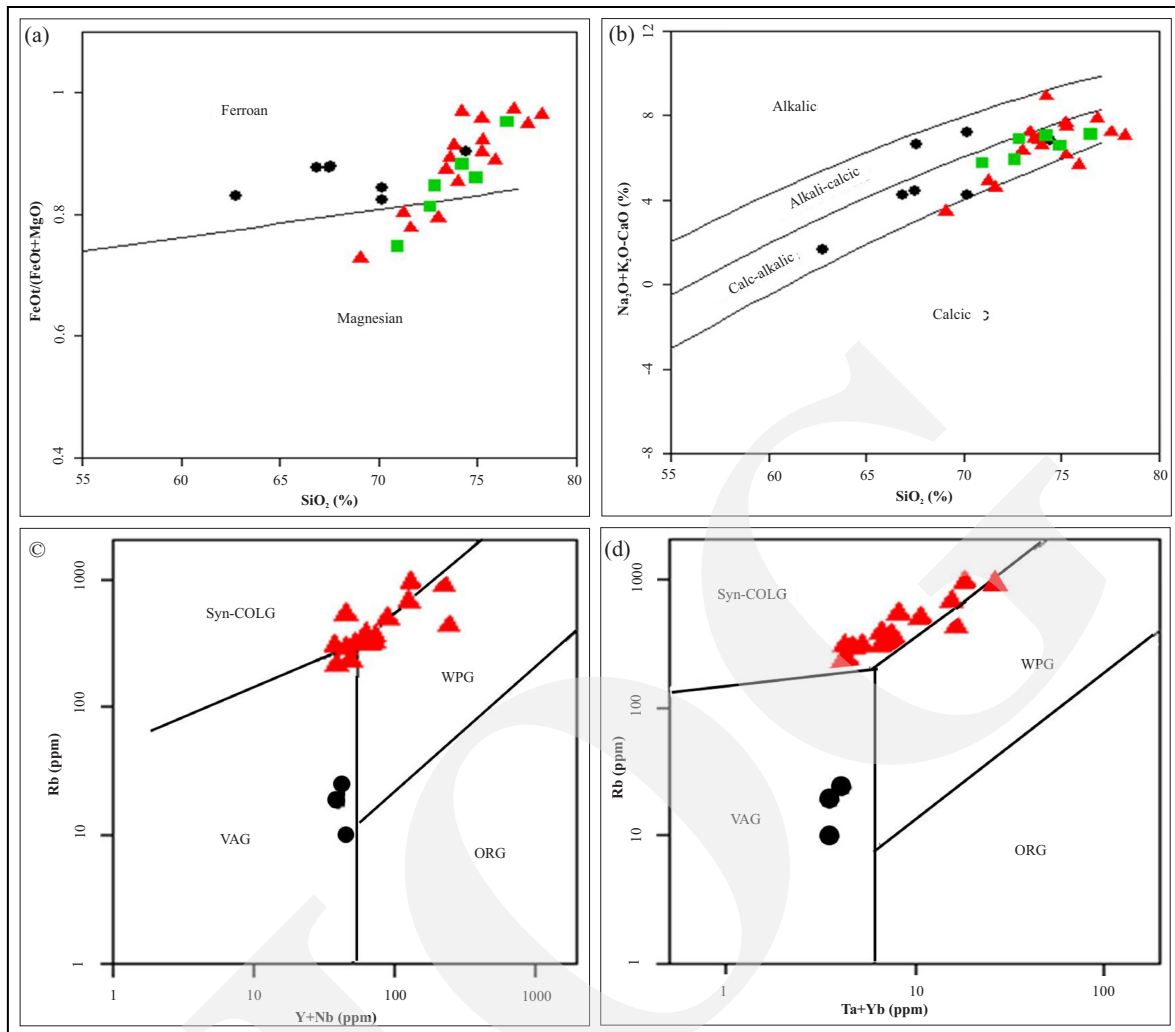


Figure 5. Plot of studied granitoids: a) All of the seven studied granitoids fall within ferroan field; b) Samples identified as calc-alkalic to alkali-calcic rocks (after Frost *et al.*, 2001); c-d) Volcanic arc associated intrusion clearly identified by both Y+Nb vs Rb and Ta+Yb vs Rb diagrams (after Pearce *et al.*, 1984). ● = Tanjung Berikat Granitoid, ■ = data from Schwartz *et al.* (1995), ▲ = data from Ng *et al.* (2017).

volcanic arc granite (VAG), within-plate granite (WPG), syn-collision granite (syn-COLG), and orogenic granites (ORG) could be distinguished. Selected granitic rocks fell into the VAG field using both Y+Nb versus Rb and Ta+Yb versus Rb diagrams emphasizing their arc-correlated nature (Figure 5c-d).

SiO₂ contents of the granitoid samples show very strong negative correlations to TiO₂, Fe₂O_{3T}, MgO, and P₂O₅ compositions with correlation coefficients (*r*) of -0.92, -0.93, -0.92, and -0.91, respectively. Na₂O and K₂O compositions rise on the decrease of SiO₂ abundance with lower correlation coefficients. On the other hand, Al₂O₃,

MnO, and CaO depict a positive correlation to SiO₂ content. The very good correlation coefficient values suggest an identical origin of the granitoid with a similar differentiation mechanism. The systematic variation of SiO₂ to other major oxides is given in Figure 6.

Trace and Rare Earth Elements

Most trace and rare earth element contents of the selected granitoids are higher than the N-type mid-ocean ridge basalt (N-MORB) value, except for Ti, Y, Yb, and Lu (Figure 7a). A prominent enrichment of several light ion lithophile elements (K, Rb, and Th) relative to some high field

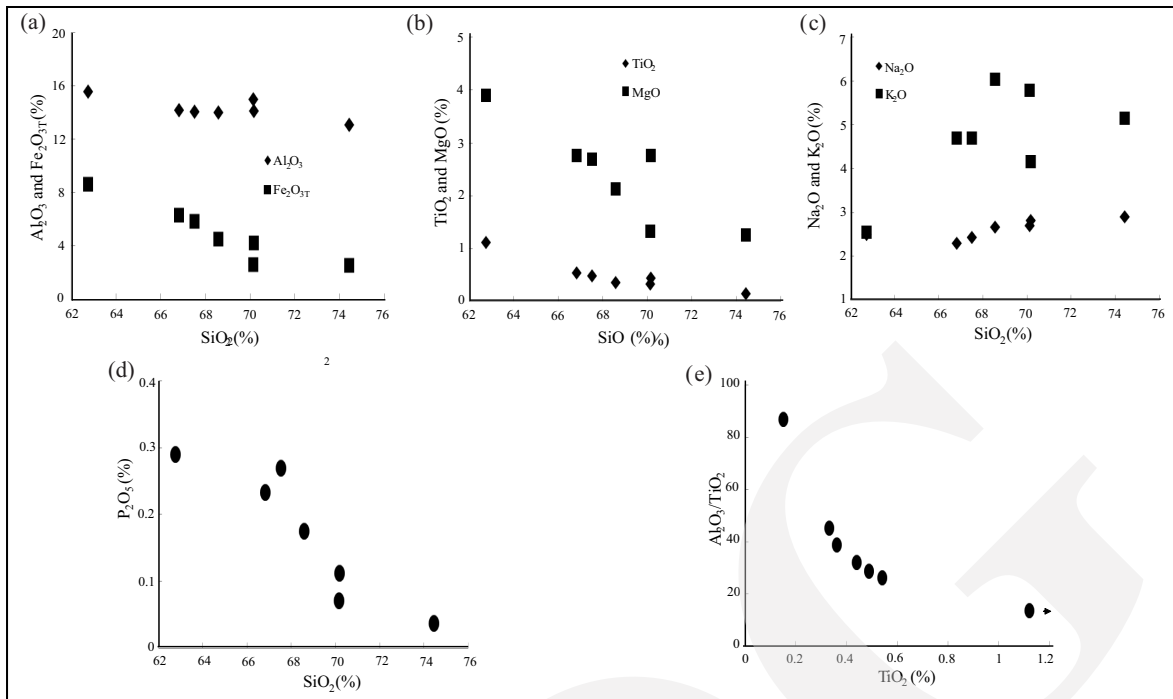


Figure 6. Bivariate plots of selected granitoid with strong to very strong correlation coefficient: a) SiO_2 versus Al_2O_3 and Fe_2O_{3T} ; b) SiO_2 versus TiO_2 and MgO ; c) SiO_2 versus Na_2O and K_2O ; d) SiO_2 versus P_2O_5 ; and e) TiO_2 versus $\text{Al}_2\text{O}_3/\text{TiO}_2$.

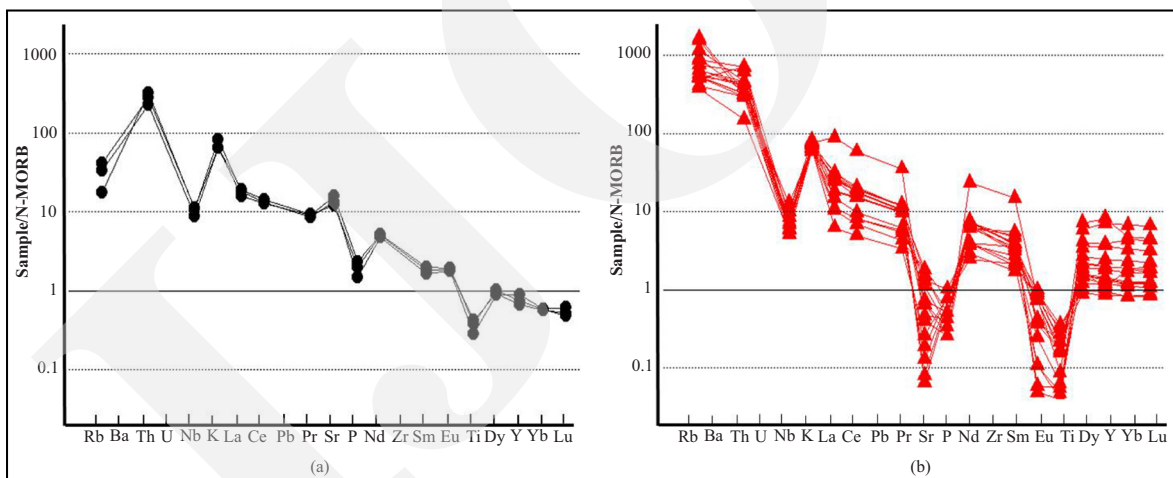


Figure 7. N-MORB (after Sun and McDonough, 1989) normalized spidergram: a) Tanjung Berikat Granitoid, and b) Other Triassic Main Range intrusions in Bangka from Ng *et al.* (2017). The diagram demonstrates a different pattern, especially on Eu anomaly and LILEs composition.

strength elements (Nb, Ti, and P) is indicated in granitoid in the N-MORB-normalized spider diagram. The graph represents positive K, Sr, and Eu anomalies and negative Nb, P, and Ti anomalies (Figure 7). Subduction related magmatic process explains LILE enrichments and negative Nb anomaly (Kaygusuz *et al.*, 2013).

Similar concave chondrite-normalized REE pattern of Tanjung Berikat Granite rocks, showing a narrow range of fractionation (La_N/Lu_N) of 18.01 – 20.61 is presented in Figure 8. The heavy-REE (HREE) profiles of the selected samples are flatter than the light-REE showing Gd_N/Lu_N and La_N/Sm_N ranges of 2.59–3.58 and 4.83–6.59, respectively. A

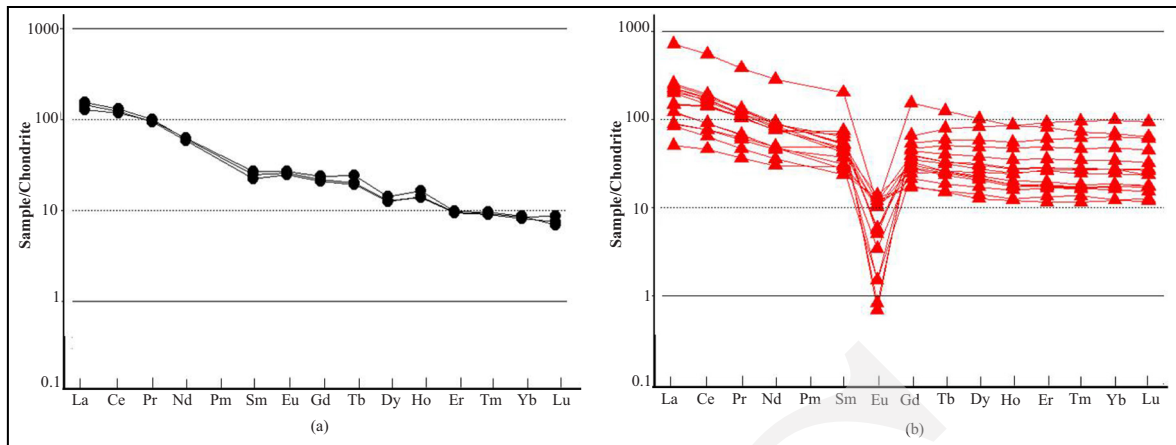


Figure 8. Chondrite (after Boynton, 1984) normalized spidergram: a) Tanjung Berikat Granitoid, and b) Other Triassic Main Range intrusions in Bangka from Ng *et al.* (2017). The two groups show dissimilarities on total REE abundance, Eu anomaly, and the degree of REE fractionation.

slight positive Eu anomaly ($Eu/Eu^* = 1.15-1.29$) of the samples could be associated with a rich-plagioclase magma source or is usually explained by plagioclase accumulation during crystallization (Irzon and Abdullah, 2016; Topuz *et al.*, 2019; Irzon *et al.*, 2020). Identical sources and similar crystallization mechanisms of the studied rock could be assumed from their analogous patterns.

DISCUSSION

Granite Classification

The low concentration of highly charged cations (Y, Nb, Zn, and Ce) in granitoids from Tanjung Berikat demonstrates a non-A-type intrusion (Irzon, 2017; Setiawan *et al.*, 2017). As directly formed by fractionation of basaltic magma or partial melting of a subducted plate, M-type granites are generally poor potassium tholeiitic rock. M-type granites are calcic and strongly metaluminous (Maurice *et al.*, 2013). Granitoids of Tanjung Berikat are not M-type according to the relatively medium to high K_2O content, medium alkalic, and metaluminous to weak peraluminous characters (Figure 4).

Muscovite as hydrated phyllosilicate mineral of aluminium and potassium are absent in the studied granites to explain their average nonperaluminous nature. A/CNK ratio of the

felsic rocks is <1.1 (1.00 on average) which is typical for I-type granite. The presence of weak peraluminous tendency in two samples implies a highly-fractionated condition or sedimentary rock incorporation during source rock melting (Chappell *et al.*, 2012; Yang *et al.*, 2020).

Granitoids from Tanjung Berikat are characterized by a remarkable SiO_2 negative correlation to P_2O_5 , pointing to the I-type nature (Figure 6d). Both in the Ta+Yb versus Rb and Yb+Nb versus Rb discriminations, all selected felsic samples plot within the volcanic-arc (VAG) field supporting an I-type intrusion in arc surroundings (Karaođlan *et al.*, 2013; Kaygusuz *et al.*, 2013; Hazad *et al.*, 2019; Irzon *et al.*, 2020). Furthermore, Tanjung Berikat Granite samples are plotted within volcanic-arc granite field of Y+Nb versus Rb and Ta+Yb versus Rb (Figure 5c and Figure 5d) diagrams. Moreover, the rocks fall within high-K calc-alkaline to shoshonitic series field in SiO_2 versus K_2O discrimination (Figure 4d). Based on these geochemical considerations, the parent I-type magma has been derived from meta-igneous rock source with some portions of lower/middle crustal or subcontinental mantle (Chappell and White, 1992; Ađlan and Altun, 2018; Kaygusuz *et al.*, 2013).

Tectonic Implication

Two granitoid samples from Tanjung Berikat give a close result of 125.5 ± 2.8 Ma and $109.4 \pm$

2.5 Ma implying crystallization age during mid-late Early Cretaceous (Table 2). However, the age acquisition data is different in relation to previous studies which explained that the S-type intrusions in Bangka Island are of Triassic age (Cobbing *et al.*, 1992; Schwartz *et al.*, 1995; Ng *et al.*, 2017). I-type characters and the Cretaceous age of the studied granitoids imply that the rocks might not belong to the Main Range Province which mostly consists of S-type granite. The Triassic intrusions are highly felsic and mostly peraluminous (Figure 4). The Main Range granites fall within the syn-collision granite field defining collision-related nature, whilst the granitoid samples of Tanjung Berikat are volcanic-arc granitoid (Figure 5).

Another problem arises from the fact that the age of Tanjung Berikat granitoid samples are distinct from most of the Eastern Province granites in Southeast Asia that emplaced during Permian to Middle Triassic (Ghani *et al.*, 2013; Oliver *et al.*, 2014; Hazad *et al.*, 2019). Arc magmatism of the samples is supported by the volcanic arc nature of the rock (Figure 5). Both high LILE/HFSE and LREE/HREE ratios of the samples point to the subduction-related setting (Muir, 1994; Liu *et al.*, 2014; Zheng, 2019). This is shown in N-MORB and primitive mantle normalized spider diagrams, respectively (Figure 7). Moreover, Nb and Ti negative anomalies strengthen the mechanism of rock emplacement. The studied granitoids are unlikely generated in the frame of Palaeo-Tethys subduction below Indochina/East Malaya as the ancient ocean was totally closed by the time of Sibumasu and Indochina/East Malaya collision in the Late Triassic (Searle *et al.*, 2012). Thus, Tanjung Berikat granitoid could probably be the result of the west-dipping subduction of Palaeo-Pacific oceanic crust beneath the eastern margin of Asia that was also reported in western Sarawak (Kirk, 1968), southwestern Kalimantan (Davies *et al.*, 2014; Hennig *et al.*, 2017), Hong Kong (Zhao *et al.*, 2017), Tioman Island, and Aur Island (Hazad *et al.*, 2019). Based on the I-type magmatism at the studied location, the Bentong-Raub suture line should be located at the west of Tanjung Berikat, and Bangka is a part of the Northeast Gondwana-

derived Indochina/East Malaya Block that is in the accordance with the previous argument (Metcalfe, 2011).

CONCLUSIONS

According to the mineralogy composition, the granitoid in Tanjung Berikat at the easternmost part of Bangka is classified as monzogranite and granodiorite. The rocks are characterized by high-K calc-alkaline to shoshonitic affinity and ferroan signature. SiO₂ bivariate plots and spider-diagrams show an identical source and differentiation mechanism of the granitoid samples. Hornblende, A/CNK ratio, SiO₂ to P₂O₅ correlation, and volcanic-arc origin of the granitoid demonstrate the I-type characteristics. High LILE/HFSE and LREE/HREE ratios coupled with Nb and Ti negative anomalies imply the arc-related tectonic setting. K-Ar dating method gave a close result of 125.5 ± 2.8 Ma and 109.4 ± 2.5 Ma implying crystallization age during mid-late Early Cretaceous.

ACKNOWLEDGMENTS

This study is funded by the Marine Geological Institute Indonesia in 2017. The authors are very grateful to Mr. Eko Partoyo, Dr. Purnama Sendjaja, and Mr. Verry E. Setiawan for the Bangka geological discussions. The assistance from Geochemistry Laboratory of the Centre for Geology Survey Indonesia in 2018, especially Mr. Kurnia Miharja is highly appreciated. The constructive comments of the anonymous reviewers are greatly acknowledged.

REFERENCES

- Açlan, M. and Altun, Y., 2018. Syn-collisional I-type Esenköy pluton (eastern Anatolia-Turkey): An indication for collision between Arabian and Eurasian plates. *Journal of African Earth Science*, 142, p.1-11.

- Barber, A.J., 2000. The origin of The Woyla Terranes in Sumatra and The Late Mesozoic evolution of the Sundaland margin. *Journal of Asian Earth Science*, 18 (6), p.713-738.
- Barber, A.J. and Crow, M.J., 2003. An evaluation of plate tectonic models for the development of Sumatra. *Gondwana Research*, 6 (1), p.1-28.
- Barber, A.J. and Crow, M.J., 2009. Structure of Sumatra and its implications for the tectonic assembly of Southeast Asia and the destruction of Paleotethys. *Island Arc*, 18 (1), p.3-20. DOI: 10.1111/j.1440-1738.2008.00631.x
- Boynton, W.V., 1984. Cosmochemistry of the rare earth elements: meteorite studies. *In: Developments in geochemistry*, p.63-114.
- Breitfeld, H.T., Hall, R., Galin, T., Forster, M.A., and BouDagher-Fadel, M.K., 2017. A Triassic to Cretaceous Sundaland-Pacific subduction margin in West Sarawak, Borneo. *Tectonophysics*, 694, p.35-56.
- Chappell, B.W. and White, A.J.R., 1992. I- and S- type granites in the Lachlan fold belt. *Transaction of the Royal Society of Edinburgh Earth Science*, 83, p.1-26.
- Chappell, B.W., Bryant, C.J., and Wyborn, D., 2012. Peraluminous I-type granites. *Lithos*, 153, p.142-153.
- Choudhury, D. and Hussain, M.F., 2021. Neoproterozoic highly fractionated I-type granitoids of Shillong Plateau, Meghalaya, Northeast India: geochemical constraints on their petrogenesis. *Acta Geochimica*, 40, p.51-66.
- Clarke, M.C.G. and Beddoe-Stephens, B., 1987. Geochemistry, mineralogy and plate tectonic setting of a Late Cretaceous Sn-W granite from Sumatra, Indonesia. *Mineralogical Magazine*, 51 (361), p.371-387.
- Cobbing, E.J., Pitfield, P.E.J., Darbyshire, D.P.F., and Mallick, D.I.J., 1992. The granites of the South-East Asian tin belt. *Overseas Memoir* 10, British Geological Survey.
- Cobbing, E.J., 2005. Granites. *Geological Society, London. Memoirs*, 31 (1), p.54-62.
- Cottam, M.A., Hall, R., and Ghani, A.A., 2013. Late Cretaceous and Cenozoic tectonics of the Malay Peninsula constrained by thermochronology. *Journal of Asian Earth Science*, 76, p.241-257. DOI:10.1016/j.jseaes.2013.04.029.
- Davies, L., Hall, R., and Armstrong, R., 2014. Cretaceous crust in SW Borneo: petrological, geochemical and geochronological constraints from the Schwaner Mountains. *Proceedings of Indonesian Petroleum Association, 38th Annual Convention and Exhibition, IPA14-G-025*.
- Frost, B.R., Barnes, C.G., Collins, W.J., Arculus, R.J., Ellis, D.J., and Frost, C.D., 2001. A geochemical classification for granitic rocks. *Journal of Petrology*, 42 (11), p.2033-2048.
- Ghani, A.A., 2000. The Western Belt granite of Peninsular Malaysia: some emergent problems on granite classification and its implication. *Geoscience Journal*, 4 (4), p.283-293.
- Ghani, A.A., Searle, M., Robb, L., and Chung, S.L., 2013. Transitional IS type characteristic in the Main Range Granite, Peninsular Malaysia. *Journal of Asian Earth Science*, 76, p.225-240. DOI:10.1016/j.jseaes.2013.05.013.
- Hall, R. and Sevastjanova, I., 2012. Australian crust in Indonesia. *Australian Journal of Earth Science*, 59 (6), p.827-844. DOI: 10.1080/08120099.2012.692335.
- Hazad, F.I., Ghani, A.A., and Lo, C.H., 2019. Arc related dioritic–granodioritic magmatism from southeastern Peninsular Malaysia and its tectonic implication. *Cretaceous Research*, 95, p.208-224.
- Hennig, J., Breitfeld, H.T., Hall, R., and Nugraha, A.S., 2017. The Mesozoic tectono-magmatic evolution at the Paleo-Pacific subduction zone in West Borneo. *Gondwana Research*, 48, p.292-310. DOI:10.1016/j.gr.2017.05.001.
- Irzon, R. and Abdullah, B., 2016. Geochemistry of Ophiolite Complex in North Konawe, Southeast Sulawesi. *Eksplorium*, 37 (2), p.101-114.
- Irzon, R., 2017. Geochemistry of Late Triassic weak Peraluminous A-Type Karimun Granite, Karimun Regency, Riau Islands Prov-

- ince. *Indonesian Journal on Geoscience*, 4 (1), p.21-37.
- Irzon, R. and Abdullah, B., 2018. Element Mobilization During Weathering Process of Ultramafic Complex in North Konawe Regency, Southeast Sulawesi Based on A Profile from Asera. *Indonesian Journal on Geoscience*, 5 (3), p.277-290.
- Irzon, R., Syafri, I., Hutabarat, J., Sendjaja, P., and Permanadewi, S., 2018. Heavy metals content and pollution in tin tailings from Singkep Island, Riau, Indonesia. *Sains Malays.*, 47 (11), p.2609-2616. DOI:10.17576/jsm-2018-4711-03.
- Irzon, R., Syafri, I., Ghani, A.A., Prabowo, A., Hutabarat, J., and Sendjaja, P., 2020. Petrography and geochemistry of the Pinkish Lagoi Granite, Bintan Island: Implication to magmatic differentiation, classification, and tectonic history. *Bulletin of Geological Society of Malaysia*, 69, p.27-37. DOI:10.7186/bgsm69202003.
- Irzon, R., Syafri, I., Suwarna, N., Hutabarat, J., Sendjaja, P., and Setiawan, V.E., 2021. Geochemistry of Granitoids in Central Sumatra: An Identification of Plate Extension during Triassic. *Geological Acta*, 19, p.1-14.
- Irzon, R., 2022. REE-Bearing Minerals in Tin Waste Dumps of Singkep Island: Geochemical Identification and Recovery. *Indonesian Journal on Geoscience*, 9 (1), p.15-26. DOI:10.17014/ijog.9.1.15-26.
- Irzon, R., Haryanto, A.D., Maryanto, S., and Hernawan, U., 2022. Distinct depositional environments of two internal reference materials with marine sediment matrix from nearby Bangka Island. *Bulletin of Geological Society of Malaysia*, 73, p.181-189. DOI:10.7186/bgsm73202215
- Jamil, A., Ghani, A.A., Zaw, K., Osman, S., and Quek, L.X., 2016. Origin and tectonic implications of the 200 Ma, collision-related Jerai pluton of the Western Granite Belt, Peninsular Malaysia. *Journal of Asian Earth Science*, 127, p.32-46. DOI:10.1016/j.jseas.2016.06.004.
- Jiang, H., Li, W.Q., Jiang, S.Y., Wang, H., and Wei, X.P., 2017. Geochronological, geochemical and Sr-Nd-Hf isotopic constraints on the petrogenesis of Late Cretaceous A-type granites from the Sibumasu Block, Southern Myanmar, SE Asia. *Lithos*, 268, p.32-47. DOI:10.1016/j.lithos.2016.11.005.
- Karaođlan, F., Parlak, O., Klötzli, U., Koller, F., and Rızaođlu, T., 2013. Age and duration of intra-oceanic arc volcanism built on a suprasubduction zone type oceanic crust in southern Neotethys, SE Anatolia. *Geoscience Frontiers*, 4 (4), p.399-408. DOI:10.1016/j.gsf.2012.11.011.
- Kaygusuz, A., Sipahi, F., Ilbeyli, N., Arslan, M., Chen, B., and Aydınçakır, E., 2013. Petrogenesis of the Late Cretaceous Turnağöl intrusion in the eastern Pontides: Implications for magma genesis in the arc setting. *Geoscience Frontiers*, 4 (4), p.423-438.
- Kazemi, K., Kananian, A., Xiao, Y., and Sarjoughian, F., 2019. Petrogenesis of Middle-Eocene granitoids and their mafic microgranular enclaves in central Urmia-Dokhtar Magmatic Arc (Iran): evidence for interaction between felsic and mafic magmas. *Geoscience Frontiers*, 10 (2), p.705-723. DOI:10.1016/j.gsf.2018.04.006.
- Kirk, H.J.C., 1968. The igneous rocks of the Sarawak and Sabah. Geological Survey Borneo Region, Malaysia, *Bulletin*, 5.
- Ko, U.K., 1986. Preliminary synthesis of the geology of Bangka Island, Indonesia. *Geosea Proceedings V. Bulletin of Geological Society of Malaysia*, 20, p.81-96.
- Liu, D., Huang, Q., Fan, S., Zhang, L., Shi, R., and Ding, L., 2014. Subduction of the Bangong–Nujiang Ocean: constraints from granites in the Bangong Co area, Tibet. *Geological Journal*, 49 (2), p.188-206.
- Liu, L., Hu, R.Z., Zhong, H., Yang, J.H., Kang, L.F., Zhang, X.C., Fu, Y.Z., Mao, W., and Tang, Y.W., 2020. Petrogenesis of multistage S-type granites from the Malay Peninsula in the Southeast Asian tin belt and their relationship to Tethyan evolution. *Gond-*

- wana Research, 84, p.20-37. DOI:10.1016/j.gr.2020.02.013.
- Loiselle, M.C. and Wones, D.R., 1979. Characteristics and origin of anorogenic granites. *Geological Society of America Abstracts with Programs*, 11, 468pp.
- Mangga, S.A. and Djamal, B., 1994. *Geological Map of the North Bangka Quadrangle, Sumatera, scale 1:250,000*. Geological Research and Development Centre, Indonesia.
- Margono, U., Supandjono, R.J.B., and Partoyo, E., 1995. *Geological Map of the South Bangka Quadrangle, Sumatera, scale 1:250,000*. Geological Research and Development Centre, Indonesia.
- Maurice, A.E., Bakhit, B.R., Basta, F.F., and Khiamy, A.A., 2013. Geochemistry of gabbros and granitoids (M-and I-types) from the Nubian Shield of Egypt: Roots of Neoproterozoic intra-oceanic island arc. *Precambrian Research*, 224, p.397-411.
- Metcalf, I., 2011. Tectonic framework and Phanerozoic evolution of Sundaland. *Gondwana Research*, 19 (1), p.3-21. DOI:10.1016/j.gr.2010.02.016.
- Metcalf, I., 2013. Tectonic evolution of the Malay Peninsula. *Journal Asian Earth Science*, 76, p.195-213. DOI:10.1016/j.jseaes.2012.12.011.
- Middlemost, E.A., 1994. Naming materials in the magma/igneous rock system. *Earth-Science Reviews*, 37 (3-4), p.215-224.
- Muir, R.J., Fitches, W.R., and Maltman, A.J., 1994. The Rhinns Complex: Proterozoic basement on Islay and Colonsay, Inner Hebrides, Scotland, and on Inishtrahull, N.W. Ireland. *Earth Environmental Science Transactions of the Royal Society Edinburgh*, 85 (1), p.77-90.
- Ng, S.W.P., Whitehouse, M.J., Roselee, M.H., Teschner, C., Murtadha, S., Oliver, G.J., Ghani, A.A., and Chang, S.C., 2017. Late Triassic granites from Bangka, Indonesia: A continuation of the main range granite province of the South-East Asian tin belt. *Journal of Asian Earth Sciences*, 138, p.548-561. DOI:10.1016/j.jseaes.2017.03.002.
- Oliver, G., Zaw, K., Hotson, M., Meffre, S., and Manka, T., 2014. U–Pb zircon geochronology of Early Permian to Late Triassic rocks from Singapore and Johor: A plate tectonic reinterpretation. *Gondwana Research*, 26 (1), p.132-143.
- Pearce, J.A., Harris, N.B., and Tindle, A.G., 1984. Trace element discrimination diagrams for the tectonic interpretation of granitic rocks. *Journal of Petrology*, 25 (4), p.956-983.
- Peccerillo, A. and Taylor, S.R., 1976. Geochemistry of Eocene calc-alkaline volcanic rocks from The Kastamonu area, northern Turkey. *Contribution to Mineralogy and Petrology*, 58 (1), p.63-81.
- Pitcher, W.S., 1983. Granite Type and Tectonic Environment. In: Hsu, K. (eds.), *Mountain Building Process*. Academic Press. London, p.19-40.
- Sarjoughian, F. and Kananian, A., 2017. Zircon U-Pb geochronology and emplacement history of intrusive rocks in the Ardestan section, central Iran. *Geological Acta*, 15 (1), p.25-36.
- Schwartz, M.O., Rajah, S.S., Askury, A.K., Puthapiban, P., and Djaswadi, S., 1995. The Southeast Asian tin belt. *Earth Science Reviews*, 38 (2-4), p.95-293.
- Searle, M.P., Whitehouse, M.J., Robb, L.J., Ghani, A.A., Hutchison, C.S., Sone, M., Ng, S.P., Roselee, M.H., Chung, S.L., and Oliver, G.J.H., 2012. Tectonic evolution of the Sibumasu–Indochina terrane collision zone in Thailand and Malaysia: constraints from new U–Pb zircon chronology of SE Asian tin granitoids. *Journal of Geological Society*, 169 (4), p.489-500. DOI:10.1144/0016-76492011-107.
- Setiawan, I., Takahashi, R., and Imai, A., 2017. Petrochemistry of granitoids in Sibolga and its surrounding areas, North Sumatra, Indonesia. *Resources Geology*, 67 (3), p.254-278. DOI:10.1111/rge.12132.
- Siregar, R.N., Widana, K.S., and Sismanto, 2022. Radiogenic heat production of S-type and I-type granite rocks in Bangka Island, Indonesia. *Kuwait Journal of Science*, 49 (3), p.1-11. DOI:10.48129/kjs.15423.

- Steiger, R.H. and Jäger, E., 1977. Subcommittee on geochronology: convention on the use of decay constants in geo- and cosmochronology. *Earth and Planetary Science Letter*, 36 (3), p.359-362.
- Streckeisen, A., 1976. To each plutonic rock its proper name. *Earth Science Reviews*, 12 (1), p.1-33.
- Sun, S.S. and McDonough, W.F., 1989. Chemical and isotopic systematics of oceanic basalts: implications for mantle composition and processes. *Geological Society, London, Special Publications*, 42 (1), p.313-345.
- Topuz, G., Candan, O., Zack, T., Chen, F., and Li, Q.L., 2019. Origin and significance of Early Miocene high-potassium I-type granite plutonism in the East Anatolian plateau (the Taşlıçay intrusion). *Lithos*, 348, 105210.
- Wang, D. and Shu, L., 2012. Late Mesozoic basin and range tectonics and related magmatism in Southeast China. *Geoscience Frontiers*, 3 (2), p.109-124. DOI:10.1016/j.gsf.2011.11.007.
- White, A.J.R., 1979. Source of Granite Magmas. *Geological Society of America Abstracts with Programs*, 11, 539pp.
- Yanbo, C. and Jingwen, M., 2010. Age and geochemistry of granites in Gejiu area, Yunnan province, SW China: constraints on their petrogenesis and tectonic setting. *Lithos*, 120 (3-4), p.258-276.
- Yang, J.H., Zhou, M.F., Hu, R.Z., Zhong, H., Williams-Jones, A.E., Liu, L., Zhang, X.C., Fu, Y.Z., and Mao, W., 2020. Granite-Related Tin Metallogenic Events and Key Controlling Factors in Peninsular Malaysia, Southeast Asia: New Insights from Cassiterite U-Pb Dating and Zircon Geochemistry. *Economic Geology*, 115 (3), p.581-601.
- Zhao, L., Wang, L., Tian, M., and Wu, F., 2017. Geochemistry and zircon U-Pb geochronology of the rhyolitic tuff on Port Island, Hong Kong: implications for early Cretaceous tectonic setting. *Geoscience Frontiers*, 8 (3), p.565-581. DOI:10.1016/j.gsf.2016.05.009.
- Zheng, Y.F., 2019. Subduction zone geochemistry. *Geoscience Frontiers*, 10 (4), p.1223-1254. DOI:10.1016/j.gsf.2019.02.003.